Cholesterol/Phospholipid Interactions in Hybrid Bilayer Membranes

Dustin Levy and Kimberly A. Briggman*

The National Institute of Standards and Technology, 100 Bureau Drive, MS8443, Gaithersburg, Maryland

Received January 23, 2007. In Final Form: April 4, 2007

The interactions between cholesterol and saturated phospholipids in hybrid bilayer membranes (HBMs) were investigated using the interface-sensitive technique of vibrational sum frequency spectroscopy (VSFS). The unique sensitivity of VSFS to order/disorder transitions of the lipid acyl chains was used to determine the main gel to liquid crystal phase transition temperature, T_m, for HBMs of binary cholesterol/phospholipid mixtures on octadecanethiolate self-assembled monolayers. The phase transition temperature and the breadth of the transition were shown to increase with cholesterol content, and the phase boundaries observed in the cholesterol/phospholipid HBMs were comparable to the published phase diagrams of binary cholesterol/phospholipid vesicles. A thermodynamic assessment of the cooperative units of the HBM phase transitions revealed the presence of <10 nm diameter domains that were independent of the cholesterol composition.

Introduction

Functional biological membranes consist of a wide array of components including saturated and unsaturated phospholipids, sphingomyelin, sterols such as cholesterol, and membrane-associated proteins.[1] The isolation of detergent-resistant domains from natural plasma membranes has led to the formulation of the lipid raft hypothesis.[2,3] Ordered domains or rafts, enriched in saturated phospholipids, cholesterol, sphingomyelin, and raft-associated proteins, are believed to contribute to cellular signaling processes. The segregation of ordered, cholesterol-rich lipid rafts from disordered, fluid phases has been detected in many model membrane systems using fluorescence microscopy,[4,5] fluorescence quenching and resonance energy transfer (FRET),[6−8] atomic force microscopy (AFM),[9−11] nuclear magnetic resonance (NMR),[12−14] electron paramagnetic resonance (EPR),[15] vibrational spectroscopies,[16−18] differential scanning calorimetry (DSC),[19−21] X-ray scattering,[22,23] and neutron scattering.[24−26] The relationships between ordered and disordered domains observed in model systems and in natural cell membranes have been discussed.[27−30]

Supported planar bilayers (SPBs) have been developed as platforms for applications in biosensing,[31,32] studies of membrane properties,[33,34] and the characterization of membrane-associated proteins.[35−37] Hybrid bilayer membranes (HBMs), composed of a phospholipid layer on top of an alkanethiolate self-assembled monolayer (SAM) attached covalently to a gold substrate, have been developed as a means of overcoming the inherent fragility of SPBs.[38] Although the use of HBMs as biosensors and platforms for biological studies has been explored, the general applicability and limitations of HBMs as models of real biological membranes have not been fully characterized.

Our laboratory has demonstrated the use of vibrational sum-frequency spectroscopy (VSFS) in the characterization of the thermal phase transitions of HBMs. We have reported that the main phase transition temperatures, T_m, of saturated phosphatidylcholine lipid layers on octadecanethiolate HBMs are approximately 10 °C higher than the transition temperatures observed for the corresponding phospholipid vesicles.[39] The consequences of such shifts in the phase transition temperatures

* To whom correspondence should be addressed. E-mail: kbriggma@nist.gov.

(1) Alberts, B.; Johnson, A.; Lewis, J.; Raff, M.; Roberts, K.; Walter, P. *Molecular Biology of the Cell*, 4th ed.; Garland Science: New York, 2002.
(2) Simons, K.; Ikonen, E. *Nature* **1997**, *387*, 569−572.
(3) Simons, K.; Toomre, D. *Nat. Rev.* **2000**, *1*, 31−41.
(4) Feigenson, G. W.; Buboltz, J. T. *Biophys. J.* **2001**, *80*, 2775−2788.
(5) Veatch, S. L.; Keller, S. L. *Phys. Rev. Lett.* **2002**, *89*, 268101.
(6) Silvius, J. R. *Biophys. J.* **2003**, *85*, 1034−1045.
(7) Fastenberg, M. E.; Shogomori, H.; Xu, X.; Brown, D. A.; London, E. *Biochemistry* **2003**, *42*, 12376−12390.
(8) London, E. *Curr. Opin. Struct. Biol.* **2002**, *12*, 480−486.
(9) Charrier, A.; Thibaudau, F. *Biophys. J.* **2005**, *89*, 1094−1101.
(10) Sanchez, J.; Badia, A. *Thin Solid Films* **2003**, *440*, 223−239.
(11) Tokumasu, F.; Jin, A. J.; Feigenson, G. W.; Dvorak, J. A. *Biophys. J.* **2003**, *84*, 2609−2618.
(12) Veatch, S. L.; Polozov, I. V.; Gawrisch, K.; Keller, S. L. *Biophys. J.* **2004**, *86*, 2910−2922.
(13) Kennedy, A.; Hmel, P. J.; Seelbaugh, J.; Quiles, J. G.; Hicks, R.; Reid, T. J. *J. Liposome Res.* **2002**, *12*, 221−237.
(14) Huang, T. H.; Lee, C. W. B.; Dasgupta, S. K.; Blume, A.; Griffin, R. G. *Biochemistry* **1993**, *32*, 13277−13287.
(15) Recktenwald, D. J.; McConnell, H. M. *Biochemistry* **1981**, *20*, 4505−4510.
(16) Pink, D. A.; Green, T. J.; Chapman, D. *Biochemistry* **1981**, *20*, 6692−6698.
(17) Volkov, V. V.; Chelli, R.; Righini, R. *J. Phys. Chem. B* **2006**, *110*, 1499−1501.
(18) Mendelsohn, R.; Liang, G. L.; Strauss, H. L.; Snyder, R. G. *Biophys. J.* **1995**, *69*, 1987−1998.
(19) Mabrey, S.; Sturtevant, J. M. *Proc. Natl. Acad. Sci. U.S.A.* **1976**, *73*, 3862−3866.
(20) Calhoun, W. I.; Shipley, G. G. *Biochemistry* **1979**, *18*, 1717−1722.
(21) McMullen, T. P. W.; Lewis, R.; McElhaney, R. N. Y. *Biochemistry* **1993**, *32*, 516−522.
(22) Hui, S. W.; He, N. B. *Biochemistry* **1983**, *22*, 1159−1164.
(23) Karmakar, S.; Raghunathan, V. A. *Phys. Rev. E* **2005**, *71*, 0619241.
(24) Knoll, W.; Schmidt, G.; Ibel, K.; Sackmann, E. *Biochemistry* **1985**, *24*, 5240−5246.
(25) Hughes, A. V.; Roser, S. J.; Gerstenberg, M.; Goldar, A.; Stidder, B.; Feidenhans'l, R.; Bradshaw, J. *Langmuir* **2002**, *18*, 8161−8171.
(26) Pencer, J.; Mills, T.; Anghel, V.; Krueger, S.; Epand, R. M.; Katsaras, J. *Eur. Phys. J. E* **2005**, *18*, 447−458.
(27) Edidin, M. *Annu. Rev. Biophys. Biomol. Struct.* **2003**, *32*, 257−283.
(28) Hancock, J. F. *Nat. Rev. Mol. Cell Biol.* **2006**, *7*, 456−462.
(29) Pike, L. J. *J. Lipid Res.* **2003**, *44*, 655−667.
(30) McMullen, T. P. W.; Lewis, R. N. A. H.; McElhaney, R. N. *Curr. Opin. Colloid Interface Sci.* **2004**, *8*, 459−468.
(31) Cornell, B. A.; Braach-Maksvytis, V. L. B.; King, L. G.; Osman, P. D. J.; Raguse, B.; Wieczorek, L.; Pace, R. J. *Nature* **1997**, *387*, 580−583.
(32) Daniel, S.; Albertorio, F.; Cremer, P. S. *MRS Bull.* **2006**, *31*, 536−540.
(33) Dietrich, C.; Bagatolli, L. A.; Volovyk, Z. N.; Thompson, N. L.; Levi, M.; Jacobson, K.; Gratton, E. *Biophys. J.* **2001**, *80*, 1417−1428.
(34) Tokumasu, F.; Hwang, J.; Dvorak, J. A. *Langmuir* **2004**, *20*, 614−618.
(35) Rao, N. M.; Silin, V.; Ridge, K. D.; Woodward, J. T.; Plant, A. L. *Anal. Biochem.* **2002**, *307*, 117−130.
(36) Yip, C. M.; Darabie, A. A.; McLaurin, J. *J. Mol. Biol.* **2002**, *318*, 97−107.
(37) Tanaka, M.; Sackmann, E. *Nature* **2005**, *437*, 656−663.
(38) Plant, A. L. *Langmuir* **1999**, *15*, 5128−5135.
(39) Anderson, N. A.; Richter, L. J.; Stephenson, J. C.; Briggman, K. A. *Langmuir* **2006**, *22*, 8333−8336.

10.1021/la070204u This article not subject to U.S. Copyright. Published 2007 by the American Chemical Society
Published on Web 05/25/2007

of HBMs will depend on the intended use; the enhanced stability of the condensed phase of the bilayer may be beneficial for some applications.

Here we investigate the effects of cholesterol on the thermal phase transition properties of saturated phospholipids in HBMs. The observed phase transition temperatures and cooperative unit sizes for binary mixtures of cholesterol and 1,2-dimyristoyl-d_{54}-*sn*-glycero-3-phosphocholine (d_{54}-DMPC) were determined as a function of the cholesterol composition from a mole fraction of 0% to a mole fraction of 25%. The results are compared to the known effects of cholesterol on the thermal properties of lipid vesicles to assess the influence of the HBM structure on the interactions between cholesterol and saturated phospholipids.

Experimental Section

Chemicals and Materials.[40] Plant-derived cholesterol and 1,2-dimyristoyl-d_{54}-*sn*-glycero-3 phosphocholine (d_{54}-DMPC) (>99%) were purchased from Avanti Polar Lipids (Alabaster, AL) as lyophilized powders. Octadecanethiol (ODT) (Fluka, ≥95%) was obtained from Sigma-Aldrich Co. (St. Louis, MO). HPLC-grade chloroform was obtained from Thermo Fisher Scientific, Inc. (Waltham, MA), and 200 proof ethanol was obtained from Warner Graham, Inc. (Cockeysville, MD). Ultrapure, deionized water (>18 MΩ) was obtained from a Nanopure Diamond Life Science water purification system from Barnstead International (Dubuque, IA). Titanium (5 nm) and gold (250 nm) coating of the glass substrate slides was performed by Platypus Technologies, LLC (Madison, WI).

Hybrid Bilayer Membrane Formation. ODT SAMs were formed on dual-track glass microaqueduct slides obtained from Bioptechs, Inc. (Butler, PA) that had been coated with gold. The gold surface was cleaned in a UV ozone oven, rinsed with ultrapure water, and recleaned in the UV ozone oven. The clean gold surface was then immersed immediately in a 200 μM ethanolic solution of ODT for at least 14 h. Formation of the ODT SAM was verified by infrared reflection−absorption spectroscopy (IRAS), ellipsometry, and VSFS. The top layer of the HBM was formed by vertical transfer of a monolayer from a Nima Technology Ltd. Langmuir−Blodgett trough (Coventry, England) to allow control of the cholesterol/phospholipid composition. Chloroform solutions of molar mixtures of cholesterol and d_{54}-DMPC were spread on a pure H_2O subphase maintained at 12 °C, and the chloroform was allowed to evaporate from the surface for 10 min. The trough barriers were then compressed at a rate of 100 cm^2/min until the surface pressure of the monolayer reached 40 mN/m. This pressure has been shown to produce ordered cholesterol/phospholipid monolayers over the concentration range used.[41,42] The monolayer was allowed to stabilize for 10 min with the surface pressure held constant. The influence of cholesterol oxidation on the phase behavior of a cholesterol/DMPC monolayer at the air−water interface has been shown to be negligible over a 20 min period,[43] and no changes in the area per molecule were observed while the trough was in constant-pressure mode. The ODT SAM was then lowered vertically through the air−water interface at a rate of 10 mm/min with the trough in constant-pressure mode. Complete transfer of the monolayer to one track of the dual-track microaqueduct slide was verified by measurement of transfer ratios (100% ± 5%). To prevent the adsorption of molecules to the second track of the slide that serves as a reference for the spectroscopic measurements, lowering of the ODT SAM through the interface was stopped, the surface pressure was reduced to 0 mN/m by opening the trough barriers, and the SAM-coated slide was dropped quickly into the subphase.

The HBMs were assembled under water into a brass variable-temperature cell with a 15 μm Teflon spacer separating the bilayer from a 2 mm thick CaF_2 window through which the laser beams passed. Care was taken to ensure that the HBM was kept in contact with water at all times and that no air bubbles were introduced into the sample cell. Ultrapure water was flowed continuously through the 15 μm gap between the HBM and the CaF_2 window during VSFS data acquisition. For phase transition studies, the temperature of the brass cell was controlled by flowing water from a thermostated water source through the cell. With each increase in temperature, the cell was allowed to stabilize for 5 min before data acquisition began. The sample temperature was monitored with a calibrated chromel−alumel thermocouple with a precision of ±0.1 °C and absolute accuracy of ±0.5 °C in contact with the back of the glass microaqueduct slide.

Vibrational Sum Frequency Spectroscopy. VSFS is a uniquely sensitive technique for the characterization of order/disorder transitions in lipid layers. Because VSFS is symmetry forbidden in systems that are locally centrosymmetric, the sum frequency signals associated with the methylene (CD_2) vibrational transitions of perdeuterated lipid acyl chains vanish when the chains are in the *all-trans* gel phase. The introduction of *gauche* defects upon transition to the liquid crystalline phase breaks the centrosymmetry of the lipid chains and allows the appearance of methylene vibrational modes in the VSFS spectrum. The increased disorder of the acyl chains also increases the disorder of the terminal methyl (CD_3) groups and causes a loss of VSFS intensity associated with CD_3 modes. Thus, the ratio of CD_2 to CD_3 VSFS intensities can be taken as a marker of order/disorder phase transitions in lipid layers. The requirement of noncentrosymmetry for the appearance of VSFS signals also makes this technique exquisitely sensitive to molecules at surfaces and interfaces and particularly well-suited to the study of HBMs.

The theory of VSFS has been described in detail.[44] Briefly, VSFS combines two incoming laser pulses, one of infrared (IR) frequency, ω_{IR}, and the other of visible (vis) frequency, ω_{vis}, at an interface or surface to produce a third beam at the sum frequency (SF), $\omega_{SF} = \omega_{IR} + \omega_{vis}$. When ω_{IR} is resonant with a vibrational transition of a molecule at the surface, the intensity of light generated at ω_{SF} is enhanced. The intensity of the VSFS signal as a function of the infrared frequency can be modeled using the following equation:

$$I_{VSFS}(\omega_{IR}) \propto \left| B + \sum_q \frac{A_q e^{i\phi_q}}{\omega_{IR} - \omega_q + i\Gamma_q} \right|^2 \quad (1)$$

The first term, B, is the nonresonant contribution to the second-order nonlinear susceptibility, $\chi^{(2)}$, due to the gold substrate. The second term represents the sum of the resonant contributions to $\chi^{(2)}$ from each vibrationally active mode, q, of molecules at the surface. The resonant contributions are modeled as Lorentzian line shapes with amplitude A_q, center frequency ω_q, line width Γ_q, and phase ϕ_q. All of the spectra reported in this paper were collected in the $P_{SF}P_{vis}P_{IR}$ polarization combination (where P polarization is defined as the electric field maximized perpendicular to the sample plane); thus, the phase between the resonant and nonresonant contributions to the VSFS intensity can vary with each resonant mode.

VSFS spectra were acquired using a nominally 50 fs Ti:sapphire laser to produce broad-bandwidth IR pulses that were overlapped in space and time at the sample surface with a copropagating, narrowed bandwidth (6 cm^{-1}) 795 nm vis pulse from a ps Ti:sapphire amplifier. The intensities, beam diameters, and incident angles were 2 μJ, 200 μm, and 67° (dry) from the surface normal for the IR beam and 20 μJ, 500 μm, and 45° (dry) from the surface normal for the vis beam. Refraction of the beams through the CaF_2 window and water changes the incident angles at the HBM surface to be roughly 43° and 32° for the IR and vis beams, respectively. All VSFS spectra were acquired under aqueous solution. The VSFS light generated at the sample surface was collected, dispersed in a spectrometer, and detected using a liquid nitrogen cooled CCD array.

(40) Certain equipment, instruments, or materials are identified in this paper to adequately specify the experimental details. Such identification does not imply recommendation by the National Institute of Standards and Technology, nor does it imply the materials are necessarily the best available for the purpose.

(41) Bonn, M.; Roke, S.; Berg, O.; Juurlink, L. B. F.; Stamouli, A.; Muller, M. *J. Phys. Chem. B* **2004**, *108*, 19083−19085.

(42) Yuan, C.; Johnston, L. J. *J. Microsc.* **2002**, *205*, 136−146.

(43) Benvegnu, D. J.; McConnell, H. M. *J. Phys. Chem.* **1993**, *97*, 6686−6691.

(44) Shen, Y. R. *Surf. Sci.* **1994**, *300*, 551−562.

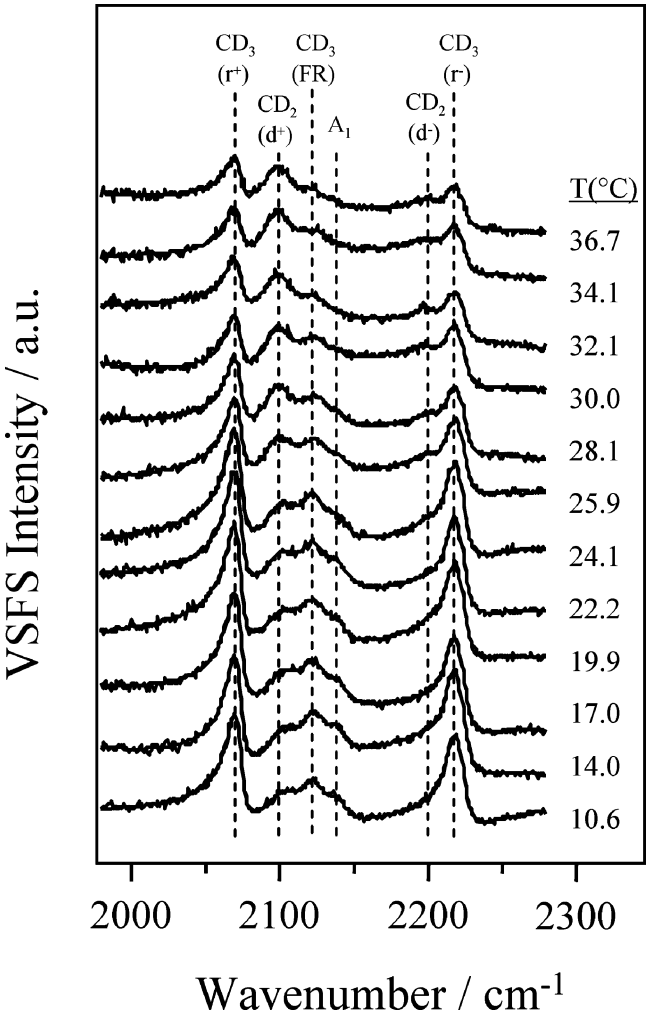

Figure 1. VSFS spectra and mode assignments of the deuterated acyl chains of d_{54}-DMPC lipid in an HBM of (d_{54}-DMPC + 5 mol % cholesterol)/ODT as a function of temperature. The spectra are offset for clarity. Smooth lines through the data are fits to eq 1.

The VSFS spectra of the deuterated acyl chains of d_{54}-DMPC were fit to six peaks on the basis of previous studies of related systems.[45,46] The gel phase frequencies and assignments for the C−D vibrational modes are CD_3 (r^+) at 2070 cm^{-1}, CD_2 (d^+) at 2100 cm^{-1}, CD_3 (FR) at 2127 cm^{-1}, A1 at 2142 cm^{-1}, CD_2 (d^-) at 2200 cm^{-1}, and CD_3 (r^-) at 2220 cm^{-1}, as labeled in Figure 1.[47] In the nonlinear least-squares fitting of the VSFS spectra according to eq 1, the vibrational frequencies were allowed to vary ±3 cm^{-1} from the assigned values, i.e., within the resolution of the experiment as determined by the bandwidth of the vis laser pulse. For facile comparison of the signal amplitudes, the widths of the CD_3 symmetric stretch (r^+), CD_2 symmetric stretch (d^+), and CD_3 Fermi resonance (FR) were held constant at 6, 10, and 10 cm^{-1}, respectively.[47] The relative amplitude of the d^+ and r^+ modes has been shown to be a marker of the degree of order/disorder of perdeuterated phospholipid chains.[39,45,48,49]

Results and Discussion

The HBMs used in this study were constructed using a fully protonated ODT underlayer and a cholesterol/d_{54}-DMPC overlayer in contact with an aqueous solution. VSFS spectra were acquired in the 1900−2300 cm^{-1} region and contain contributions from only the deuterated acyl chains of d_{54}-DMPC. Figure 1 shows the VSFS spectra of a d_{54}-DMPC/ODT HBM with 5 mol % cholesterol in the upper layer as a function of temperature. When the temperature is less than 28 °C, the VSFS spectra are consistent with ordered acyl phospholipid chains in an *all-trans* configuration, which results in near cancellation of the VSFS signals from CD_2 resonances.[50] At temperatures exceeding 28 °C the intensity of the CD_2 symmetric stretch (d^+) increases due to the introduction of *gauche* defects that break the centrosymmetry of the CD_2 modes of the acyl phospholipid chains. The increase in disorder of the phospholipid chains is also accompanied by a decrease in the VSFS intensity of the CD_3 symmetric stretch (r^+).

The VSFS spectra in Figure 1 were fit to eq 1 to extract the amplitudes of the d^+ and r^+ modes. These amplitudes were ratioed (d^+/r^+) and used as a quantitative measure of the degree of disorder in the upper layer of the HBM. The temperature dependence of d^+/r^+ was analyzed according to a sigmoid function, $S = C + A/(1 + \exp[(T_m - T)/D])$, in which C, A, T_m, and D were the unknown parameters recovered from the experimental data. In the sigmoid model function, S is the d^+/r^+ ratio, C is the value of d^+/r^+ at the low-temperature limit, A is the magnitude of the change in d^+/r^+ between the low-temperature and high-temperature limits, T_m is the midpoint temperature of the phase transition, and D is a width factor related to the enthalpy and cooperative unit size of the transition.[51] The d^+/r^+ ratios extracted from the VSFS spectra of three d_{54}-DMPC/ODT HBM samples with 5 mol % cholesterol are included in Figure 2b. A sigmoidal fit to the temperature dependence of d^+/r^+ from three experiments gives $T_m = 28.2 \pm 1.0$ °C and $D = 1.86 \pm 0.69$ °C.[52]

Temperature-dependent VSFS spectra of a d_{54}-DMPC/ODT HBM with 25 mol % cholesterol are shown in Figure 3. Comparison of Figures 1 and 3 reveals two significant differences. First, ordered phospholipid chains persist at higher temperatures when the cholesterol content is raised from 5 to 25 mol %. Second, the breadth of the phase transition, i.e., the temperature range over which the transition occurs, is larger for HBMs containing 25 mol % cholesterol. The d^+/r^+ ratios extracted from fits to VSFS spectra from three d_{54}-DMPC/ODT HBMs with 25 mol % cholesterol are presented in Figure 2f. A sigmoidal fit to the temperature dependence of d^+/r^+ from three experiments gives $T_m = 40.3 \pm 1.4$ °C and $D = 5.15 \pm 0.80$ °C.

VSFS spectra were also collected for pure d_{54}-DMPC/ODT HBMs and HBMs containing 10, 15, and 20 mol % cholesterol. The d^+/r^+ ratios determined at each of these compositions are plotted as a function of temperature in Figure 2. The transition

(45) Anderson, N. A.; Richter, L. J.; Stephenson, J. C.; Briggman, K. A. *J. Am. Chem. Soc.* **2007**, *129*, 2094−2100.

(46) Yang, C. S. C.; Richter, L. J.; Stephenson, J. C.; Briggman, K. A. *Langmuir* **2002**, *18*, 7549−7556.

(47) These parameters differ slightly from those used to fit related spectra in ref 45. Identical conclusions are drawn from the analysis of the VSFS spectra using either set of parameters. We ascribe no physical significance to the differences in these parameter sets at this time.

(48) Gurau, M. C.; Castellana, E. T.; Albertorio, F.; Kataoka, S.; Lim, S. M.; Yang, R. D.; Cremer, P. S. *J. Am. Chem. Soc.* **2003**, *125*, 11166−11167.

(49) Roke, S.; Schins, J.; Muller, M.; Bonn, M. *Phys. Rev. Lett.* **2003**, *90*, 128101.

(50) The relative intensity of the CD_2 d^+ mode in the *all-trans* gel phase appears to be larger than that observed for the CH_2 d^+ mode for the gel phase of a protonated phospholipid monolayer. This has been previously reported in ref 45 for gel phase perdeuterated lipid monolayers of HBMs. This difference is also observed for PPP spectra of crystalline perdeuterated ODT SAMs on gold (ref 46).

(51) Kirchhoff, W. H.; Levin, I. W. *J. Res. Natl. Bur. Stand.* **1987**, *92*, 113−128.

(52) As described in ref 51, sigmoidal fits to the inverse ratio r^+/d^+ will give apparent phase transition temperatures different from those obtained from analysis of the d^+/r^+ ratios. For the 5 mol % cholesterol d_{54}-DMPC/ODT HBM, the T_m extracted from sigmoidal fits to the ratio r^+/d^+ is 2.6 °C less than that extracted from sigmoidal fits to the ratio d^+/r^+. The magnitude of the inverse shift in the phase transition temperature increases with the scale factor D, i.e., with the concentration (mol %) of cholesterol in the HBM, but the conclusions drawn in this paper remain unchanged.

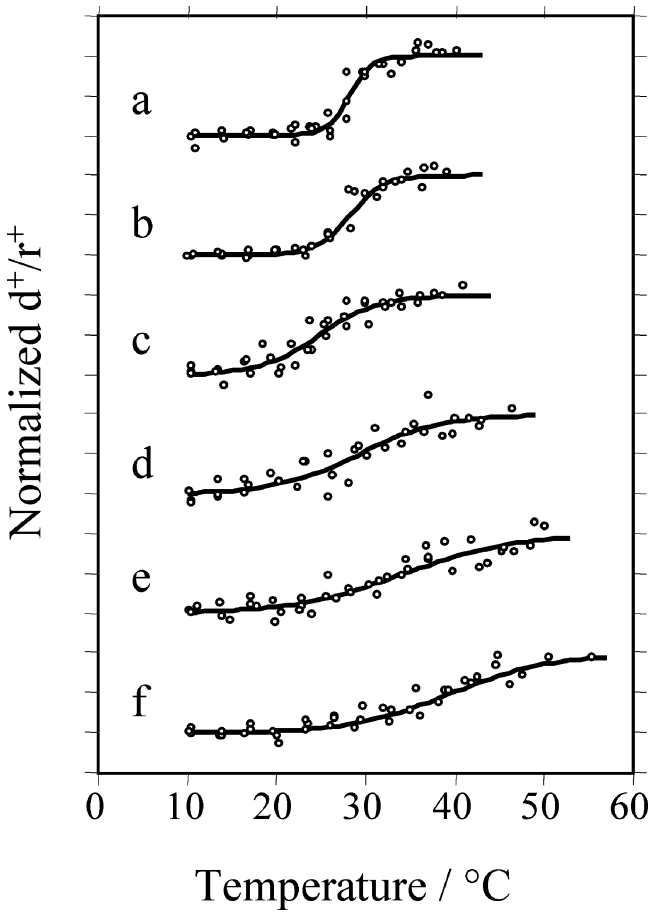

Figure 2. Ratios of the d^+/r^+ amplitudes extracted from the VSFS spectra of d_{54}-DMPC/ODT HBMs with (a) 0 mol % cholesterol, (b) 5 mol % cholesterol, (c) 10 mol % cholesterol, (d) 15 mol % cholesterol, (e) 20 mol % cholesterol, and (f) 25 mol % cholesterol in the d_{54}-DMPC layer as a function of temperature. The data points are from three independent experiments for each composition, and the solid curves are averaged sigmoidal fits for the three experiments. For clarity, the data for each composition are normalized on the basis of the change in amplitude of the d^+/r^+ ratio between the low- and high-temperature limits, as determined from the sigmoidal fits.

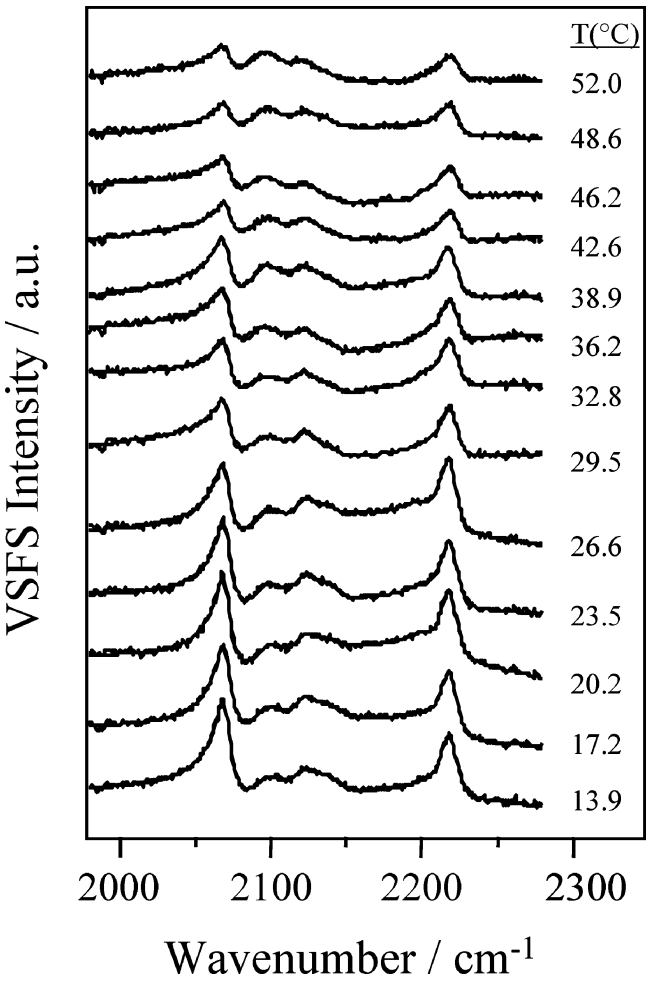

Figure 3. VSFS spectra of the deuterated acyl chains of d_{54}-DMPC lipid in an HBM of (d_{54}-DMPC + 25 mol % cholesterol)/ODT as a function of temperature. The spectra are offset for clarity. Smooth lines through the data are fits to eq 1.

temperatures and width factors determined for each composition are summarized in Table 1.

Our laboratory has reported a transition temperature $T_m = 28.3 \pm 0.7$ °C for a d_{54}-DMPC/ODT HBM in a previous paper.[39] In that study, the upper phospholipid layer of the HBM was introduced by vesicle fusion to the ODT SAM. In contrast, the HBMs used in the present study were formed by monolayer transfer from a Langmuir−Blodgett trough to an ODT SAM. Film transfer is a preferred method for the formation of HBMs containing multiple lipid or sterol components because the relative compositions of materials introduced to the HBM can be better controlled. The transition temperature of the d_{54}-DMPC/ODT HBM produced by film transfer, $T_m = 28.2 \pm 0.9$ °C (Table 1), matches the transition temperature of the same HBM produced by vesicle fusion. This result indicates that HBMs formed using either method have similar thermal properties.

The phase transition temperatures of saturated phosphocholine lipid layers on octadecanethiolate HBMs are approximately 10 °C higher than the transition temperatures observed for the corresponding phospholipid vesicles.[39] Our laboratory has demonstrated that the phase transition temperature of the upper phospholipid layer of the HBM can be controlled by changing the chemistry of the underlying SAM.[45] Introduction of disorder into the underlayer of the HBM eliminated the 10 °C shift to higher temperatures in the T_m of the phospholipid overlayer. Thus, different HBM underlayers can be chosen for specific applications. For the present study of binary cholesterol/phospholipid HBMs, the ODT SAM was chosen to prevent the partitioning of cholesterol between the upper and lower layers of the HBM, which would complicate our analysis. The ODT SAM has been shown previously to be crystalline and impenetrable at all temperatures relevant to the current work.[45]

Table 1. Thermal Properties of d_{54}-DMPC/ODT HBMs with Different Cholesterol Compositions in the Upper Layer of the Membrane[a]

cholesterol concn (mol %)	T_m (°C)	D (°C)	T_{10} (°C)	T_{90} (°C)
0	28.2 ± 0.9	1.25 ± 0.49	25.5 ± 1.5	31.0 ± 1.5
5	28.2 ± 1.0	1.86 ± 0.69	24.1 ± 1.8	32.3 ± 1.8
10	24.8 ± 1.9	3.26 ± 0.94	17.6 ± 2.8	32.0 ± 2.8
15	29.2 ± 3.3	4.64 ± 1.25	19.0 ± 4.3	39.4 ± 4.3
20	34.1 ± 2.0	6.17 ± 1.39	20.5 ± 3.7	47.7 ± 3.7
25	40.3 ± 1.4	5.15 ± 0.80	29.0 ± 2.2	51.6 ± 2.2

[a] Uncertainties are expressed as the standard deviation of three experiments.

Influence of Cholesterol on the HBM Phase Behavior. The melting curves of d_{54}-DMPC/ODT HBMs are affected significantly by the introduction of increasing amounts of cholesterol (Figure 2). The trends in T_m and D show that the phase transition

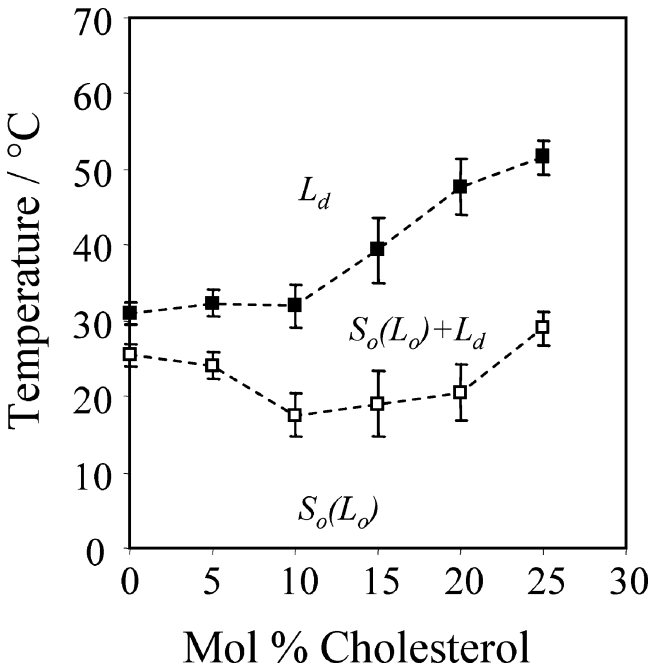

Figure 4. Partial phase diagram for cholesterol containing d_{54}-DMPC/ODT HBMs plotted versus the concentration (mol %) of cholesterol in the upper layer of the membrane. Plotted are the onset (T_{10}, open squares) and end points (T_{90}, closed squares) of the phase transition as determined by VSFS. The dashed lines connecting the points are meant to guide the eye and are not fits to the data. The notation $S_o(L_o)$ indicates uncertainty in the assignment of the solid ordered and liquid ordered phases.

temperature varies by ∼15 °C and the width of the transition varies by a factor of ∼5 over the range of 0−25 mol % cholesterol (Table 1). The onset of the melting phase transition, T_{10}, can be defined as the temperature at which the ratio d^+/r^+ reaches 10% of its maximum change in amplitude. T_{10} can be expressed quantitatively as a function of T_m and D using the expression $T_{10} = T_m - D \ln 9$. Similarly, the end point of the phase transition, T_{90}, is defined as the temperature at which the ratio d^+/r^+ reaches 90% of its maximum amplitude change and is given by the expression $T_{90} = T_m - D \ln(1/9)$. The use of T_{10} and T_{90} values to define the onset and end point of a phase transition and their relationship to the transition enthalpy and cooperativity have been discussed.[53] The T_{10} and T_{90} values determined at each HBM composition are included in Table 1 and plotted versus the concentration (mol %) of cholesterol in Figure 4.

The phase behavior of binary cholesterol/saturated phospholipid mixtures as a function of temperature and composition has been studied experimentally[53−57] and modeled theoretically.[54,58] The phase boundaries plotted in Figure 4 show three notable similarities to the phase boundaries reported for binary cholesterol/saturated phospholipid vesicles. First, the negative slope of the lower phase boundary line between 0 and 10 mol % cholesterol observed in Figure 4 has also been detected in differential scanning calorimetry (DSC) traces of binary cholesterol/phosphatidylcholine vesicles.[54,56] Second, the positive slope of the lower phase boundary at >20 mol % cholesterol has been identified in NMR and EPR studies.[15,54,56] Finally, the positive slope of the upper phase boundary between 10 and 20 mol % cholesterol has also been demonstrated in DSC traces and EPR spectra of binary cholesterol/phosphatidylcholine vesicles.[15,54,56]

Given the observed similarities between the phase behavior of HBMs and vesicles containing binary mixtures of cholesterol and saturated phospholipids, it is concluded that the lateral interactions between cholesterol and d_{54}-DMPC are similar in both bilayer systems. The sensitivity of VSFS to order/disorder transitions allows assignment of the region above the T_{90} line as a disordered phase, the region below the T_{10} line as an ordered phase, and the region between the T_{10} and T_{90} lines as coexisting ordered and disordered phases. In keeping with the notation accepted in the literature, the uppermost region in Figure 4 is labeled as a disordered liquid crystal, L_d, phase. The region below the T_{10} line is likely more complicated. Previously published phase diagrams of binary cholesterol/saturated phospholipid vesicles have identified a solid ordered, S_o, phase at low cholesterol concentrations (<8 mol %), coexisting S_o and liquid ordered, L_o, phases at intermediate cholesterol concentrations (8−25 mol %), and a single L_o phase at cholesterol concentrations exceeding 25 mol %.[54−57] In the L_o phase, the conformational order of the acyl phospholipid chains is characteristic of the S_o phase, but the lateral mobility of the phospholipids is characteristic of the L_d phase. VSFS is not sensitive to changes in lateral mobility and, therefore, cannot distinguish the S_o and L_o phases. The low-temperature region in Figure 4 is labeled as $S_o(L_o)$ to indicate uncertainty in our assignment of solid ordered and liquid ordered phases. Similarly, both coexisting S_o and L_d and coexisting L_o and L_d phases have been proposed to exist in the region bound by the T_{10} and T_{90} lines in Figure 4.[56,59]

Analysis of Transition Enthalpies and Cooperative Unit Sizes. Observations of coexisting ordered and disordered domains in model membrane systems continue to be of interest due to the proposed existence of functional lipid rafts in biological membranes. The domain sizes that have been reported in the literature for artificial and natural membranes have ranged from a few nanometers to hundreds of micrometers.[28,60] Measurements of membrane domains are often conducted directly using fluorescence microscopy, FRET, or AFM[8,11,12,34,61] or indirectly from phase transitions detected using DSC and vibrational spectroscopy.[19,62−65]

For a two-state process, i.e., a transition from an ordered phase to a disordered phase, the effective domain size, n_{eff}, or cooperative unit size, is given by the van't Hoff transition enthalpy, ΔH_{vH}, divided by the calorimetric enthalpy, ΔH_{cal},[64] i.e., $n_{eff} = \Delta H_{vH}/\Delta H_{cal}$. The analysis of the traces in Figure 2 gives the product of the calorimetric enthalpy and the cooperative unit size according to $\Delta H_{cal} n_{eff} = (RT_m^2)/D$, where R is the gas constant.[51,66] Table 2 gives the values of $\Delta H_{cal} n_{eff}$ determined at each cholesterol/d_{54}-DMPC composition from the parameters T_m and D in Table 1. The observed trend indicates that the calorimetric enthalpy and/or the cooperative unit size must decrease upon the addition of increasing amounts of cholesterol to the HBM.

(53) Hinz, H. J.; Sturtevant, J. M. *J. Biol. Chem.* **1972**, *247*, 3697−3700.
(54) Ipsen, J. H.; Karlstrom, G.; Mouritsen, O. G.; Wennerstrom, H.; Zuckerman, M. J. *Biochim. Biophys. Acta* **1987**, *905*, 162−172.
(55) Thewalt, J. L.; Bloom, M. *Biophys. J.* **1992**, *63*, 1176−1181.
(56) Vist, M. R.; Davis, J. H. *Biochemistry* **1990**, *29*, 451−464.
(57) Almeida, P. F. F.; Vaz, W. L. C.; Thompson, T. E. *Biochemistry* **1992**, *31*, 6739−6747.
(58) Nielsen, M.; Miao, L.; Ipsen, J. H.; Zuckermann, M. J.; Mouritsen, O. G. *Phys. Rev. E* **1999**, *59*, 5790−5803.
(59) McMullen, T. P. W.; McElhaney, R. N. *Biochim. Biophys. Acta* **1995**, *1234*, 90−98.
(60) Bloom, M.; Thewalt, J. L. *Mol. Membr. Biol.* **1995**, *12*, 9−13.
(61) Gliss, C.; Clausen-Schaumann, H.; Gunther, R.; Odenbach, S.; Randi, O.; Bayerl, T. M. *Biophys. J.* **1998**, *74*, 2443−2450.
(62) Mellier, A.; Kanza, J. *J. Chim. Phys. Phys.-Chim. Biol.* **1994**, *91*, 1507−1518.
(63) Yellin, N.; Levin, I. W. *Biochim. Biophys. Acta* **1977**, *468*, 490−494.
(64) Hinz, H. J.; Sturtevant, J. M. *J. Biol. Chem.* **1972**, *247*, 6071−6075.
(65) Mellier, A.; Ech-Chahoubi, A.; Le Roy, A. *J. Chim. Phys. Phys.-Chim. Biol.* **1993**, *90*, 51−62.
(66) Tokumasu, F.; Jin, A. J.; Dvorak, J. A. *Jpn. Soc. Electron Microsc.* **2002**, *51*, 1−9.

Table 2. Transition Enthalpies and Cooperative Unit Sizes of d_{54}-DMPC/ODT HBMs with Different Cholesterol Compositions in the Upper Layer of the Membrane[a]

cholesterol concn (mol %)	$\Delta H_{cal} n_{eff}$ ((kJ·molecule)/mol)	ΔH_{cal}[b] (kJ/mol)	n_{eff} (molecules)
0	669 ± 255	16.3	41 ± 16
5	456 ± 205	13.4	34 ± 15
10	238 ± 75	10.5	23 ± 7
15	172 ± 42	8.4	21 ± 5
20	146 ± 71	6.3	23 ± 11
25	159 ± 25	5.0	32 ± 5

[a] Uncertainties are expressed as the standard deviation of three experiments. [b] Transition enthalpies taken from differential scanning calorimetry measurements of cholesterol/DMPC vesicles[21] and adjusted for the deuterium isotope effect for the transition enthalpy of d_{54}-DMPC.[70]

There have been several reports of the cholesterol dependence of the calorimetric enthalpies of binary cholesterol/phospholipid vesicles.[20,21,53,67−69] All of these results show that ΔH_{cal} decreases with increasing cholesterol content in the 0−25 mol % range. Absolute calorimetric enthalpies were taken from a thorough study of cholesterol/DMPC vesicles[21] and adjusted to account for the deuterium isotope effect of the d_{54}-DMPC lipids used here.[70] The adjusted calorimetric enthalpies are included in Table 2 along with the determinations of the cooperative unit sizes. The cooperative units fall in the range of 15−60 molecules and exhibit no clear dependence on the cholesterol concentration. Therefore, it appears that the obvious changes in the breadths of the phase transitions in Figure 2, as well as the trend in the products $\Delta H_{cal} n_{eff}$, can be accounted for solely by changes in the calorimetric enthalpies of cholesterol/phospholipid mixtures.

Because the determination of T_m and D gives only the product $\Delta H_{cal} n_{eff}$ instead of the direct value of the cooperative unit size, errors in the values of the calorimetric enthalpies will impact the calculated values of n_{eff}. For example, the calorimetric enthalpies of vesicles and HBMs consisting of the same materials may not be identical. A recent DSC study of mica-supported phosphocholine bilayers, however, gave a transition enthalpy comparable to that observed for vesicles of the same phospholipids.[71] For our purposes, we have assumed that the absolute calorimetric enthalpies of octadecanethiolate HBMs are also comparable to those of vesicles and that the cholesterol dependence of ΔH_{cal} is also identical in both systems. Justification of the latter assumption comes from the observed similarities between the partial HBM phase diagram plotted in Figure 4 and published phase diagrams of binary cholesterol/saturated phospholipid vesicles.

A collection of cooperative unit sizes reported in the literature for DMPC vesicles and supported bilayers based on the evaluation of van't Hoff transition enthalpies is presented in Table 3. The reported cooperative units range 2 orders of magnitude from approximately 20 molecules to almost 2000 molecules. Multilamellar vesicles tend to have the largest cooperative units, and the variation in the observed unit sizes is likely due to the sample preparation conditions and the presence of impurities.[72] Large

Table 3. Reported Cooperative Unit Sizes for DMPC Bilayers and Multilayers

size (molecules)	system[a]	method[b]	ref
1720 ± 120	MLV	DSC	80
1700	MLV	DSC	81
369	MLV	DSC	73
330	MLV	DSC	19
200 ± 40	MLV	DSC	64
195 ± 32	mica-supported	*T*-controlled AFM	76
90	MLV	IR	62
67	LUV	DSC	73
35−45	mica-supported	*T*-controlled AFM	82
30	SUV	DSC	73
18−75	mica-supported	*T*-controlled AFM	66
15−60	HBM	VSFS	this work

[a] MLV = multilamellar vesicle, LUV = large unilamellar vesicle, SUV = small unilamellar vesicle, and HBM = hybrid bilayer membrane. [b] DSC = differential scanning calorimetry, *T*-controlled AFM = temperature-controlled atomic force microscopy, IR = infrared spectroscopy, VSFS = vibrational sum frequency spectroscopy.

and small unilamellar vesicles give smaller cooperative units; however, the unit sizes in these cases are influenced heavily by curvature effects and the finite sizes of the vesicles.[73−75] Mica-supported DMPC bilayers give relatively low cooperative unit sizes ranging from approximately 20 to 200 molecules, as determined by temperature-controlled AFM.[66,76] The AFM result of $n_{eff} = 18-75$[66] was obtained assuming the calorimetric enthalpy of the supported DMPC bilayer was identical to that of the DMPC vesicles; however, the authors noted that AFM images indicated domain sizes on a much larger scale than tens of molecules. It was suggested that the n_{eff} value may represent the unit size for lateral cooperativity, which leads to the larger domains observed by AFM. In contrast, in another AFM experiment, the result of $n_{eff} = 195 \pm 32$[76] was obtained directly from AFM images and then used to calculate ΔH_{cal} for the supported bilayer. In this case, the calculated transition enthalpy exceeded that of the DMPC vesicles by nearly a factor of 2. These contrasting interpretations of the phase behavior of supported bilayers demonstrate the uncertainty that arises when attempts are made to separate ΔH_{cal} and n_{eff} from the van't Hoff transition enthalpy.

Our present result of $n_{eff} = 15-60$ molecules, based on the error limits in Table 2, for octadecanethiolate HBMs containing cholesterol and d_{54}-DMPC is consistent with the cooperative unit sizes reported for mica-supported DMPC and suggests that small domain sizes are a characteristic feature of supported bilayers. The observation that the cooperative unit size is independent of the cholesterol concentration merits comment. A recent AFM and near-field scanning optical microscopy (NSOM) study demonstrated that the domain structure of cholesterol/phospholipid monolayers deposited on mica was influenced by the cholesterol composition of the monolayer.[42] However, the domain sizes observed in these images are still larger than the tens-of-molecules scale inferred from calorimetric measurements, and the relationship between these two scales is not known. The inherent uncertainties associated with the determination of cooperative unit sizes from van't Hoff transition enthalpies make it difficult to measure small, cholesterol-induced changes in

(67) Estep, T. N.; Mountcastle, D. B.; Biltonen, R. L.; Thompson, T. E. *Biochemistry* **1978**, *17*, 1984−1989.
(68) Mabrey, S.; Mateo, P. L.; Sturtevant, J. M. *Biochemistry* **1978**, *17*, 2464−2468.
(69) Lentz, B. R.; Barrow, D. A.; Hoechli, M. *Biochemistry* **1980**, *19*, 1943−1954.
(70) Guard-Friar, D.; Chen, C. H.; Engle, A. S. *J. Phys. Chem.* **1985**, *89*, 1810−1813.
(71) Yang, J.; Appleyard, J. *J. Phys. Chem. B* **2000**, *104*, 8097−8100.
(72) Koberl, M.; Schoppe, A.; Hinz, H. J.; Rapp, G. *Chem. Phys. Lipids* **1998**, *95*, 59−82.
(73) Kodama, M.; Miyata, T.; Takaichi, Y. *Biochim. Biophys. Acta* **1993**, *1993*, 90−97.
(74) Marsh, D.; Watts, A.; Knowles, P. F. *Biochim. Biophys. Acta* **1977**, *465*, 500−514.
(75) Nagano, H.; Nakanishi, T.; Yao, H.; Ema, K. *Phys. Rev. E* **1995**, *52*, 4244−4250.
(76) Enders, O.; Ngezahayo, A.; Wiechmann, M.; Leisten, F.; Kolb, H. A. *Biophys. J.* **2004**, *87*, 2522−2531.

cooperativity that may lead to large, visualizable domain structures in lipid bilayers.

The cross-sectional area of a DMPC molecule in a liquid disordered phase is 0.6 nm^2.[66] Assuming the cooperative unit describes a cylindrical, phospholipid-rich domain, the domain diameters observed in the cholesterol/d_{54}-DMPC HBMs are estimated to be 5 ± 2 nm. While the estimated domain diameters would be smaller if cholesterol molecules were included, this effect is small compared to the experimental uncertainty. Domain sizes of less than 10 nm have also been observed in recent experimental studies and theoretical simulations of binary phospholipid bilayers.[61,77,78] How phase segregation on this scale may be relevant to biological processes in natural membranes remains an open question.[79]

Conclusions

We have investigated for the first time the phase behavior of HBMs containing binary mixtures of cholesterol and saturated phospholipids. The sensitivity of VSFS to order/disorder transitions was used to determine the main gel to liquid crystal phase transition temperatures of the HBMs as a function of cholesterol composition. The phase boundaries observed for the HBMs were consistent with published phase diagrams of binary cholesterol/saturated phospholipid vesicles, which suggests that the lateral interactions between cholesterol and phospholipids are similar in both systems. An analysis of the observed phase transitions in terms of the classical van't Hoff formalism yielded cooperative unit sizes of less than 10 nm diameter. These domain sizes are comparable to those observed in other types of supported bilayers, and knowledge of these domains could prove useful in future studies of biomolecular interactions on HBM platforms.

Acknowledgment. D.L. acknowledges the National Research Council for postdoctoral fellowship support.

LA070204U

(77) Michonova-Alexova, E. I.; Sugar, I. P. *J. Phys. Chem. B* **2001**, *105*, 10076−10083.
(78) Sugar, I. P.; Michonova-Alexova, E. I.; Chong, P. L. G. *Biophys. J.* **2001**, *81*, 2425−2441.
(79) Nicolau, D. V., Jr.; Burrage, K.; Parton, R. G.; Hancock, J. F. *Mol. Cell. Biol.* **2006**, *26*, 313−323.
(80) Sturtevant, J. M. *Chem. Phys. Lipids* **1998**, *95*, 163−168.
(81) Knoll, W. *Thermochim. Acta* **1984**, *77*, 35−47.
(82) Xie, A. F.; Yamada, R.; Gewirth, A. A.; Granick, S. *Phys. Rev. Lett.* **2002**, *89*, 246103.